Title

Biogenic sulfide control by nitrate and (per)chlorate – A monitoring and modeling investigation

Authors

Wu, Yuxin
Cheng, Yiwei
Hubbard, Christopher G
et al.

Publication Date

2018

DOI

10.1016/j.chemgeo.2017.11.016

Peer reviewed

Chemical Geology 476 (2018) 180–190

Contents lists available at ScienceDirect

Chemical Geology

journal homepage: www.elsevier.com/locate/chemgeo

Biogenic sulfide control by nitrate and (per)chlorate – A monitoring and modeling investigation

Yuxin Wu[a,*], Yiwei Cheng[a], Christopher G. Hubbard[b,1], Susan Hubbard[a], Jonathan B. Ajo-Franklin[b]

[a] Climate and Ecosystem Sciences Division, Lawrence Berkeley National Laboratory, 1 Cyclotron Rd, Berkeley, CA 94720, USA
[b] Energy Geosciences Division, Lawrence Berkeley National Laboratory, 1 Cyclotron Rd, Berkeley, CA 94720, USA

ARTICLE INFO

Editor: K Johannesson

Keywords:
Biosouring
Souring control
Galvanic potential
Reactive transport modeling

ABSTRACT

Biosouring is commonly encountered during secondary oil recovery when seawater or another high sulfate water source is utilized for flooding; as a result, effective souring control is of great interest to the oil industry. Here we describe a laboratory study to evaluate the relative effectiveness of souring interventions through the injection of nitrate, chlorate and perchlorate, collectively (per)chlorate, solutions and whether in-situ galvanic potential measurements can be used for convenient and quantitative tracking of sulfide dynamics. Nitrate has typically been the chemical of choice for souring treatments, while the efficacy of (per)chlorate as a new candidate inhibitor has only been explored recently. (Per)chlorate is known to inhibit oil reservoir souring via mechanisms such as toxicity, bio-competitive exclusion and sulfur redox cycling. Two sets of experiments under different matrix and inoculation conditions were conducted to evaluate treatment efficiency under variable baseline physical and biogeochemical conditions. Our data demonstrated the sensitivity of the galvanic potential signals to sulfide concentrations where the sulfide-galvanic potential correlation is similar to the theoretical predictions based on the Nernst equation, demonstrating the feasibility of using galvanic potential as a quick and economical method for quantifying in situ sulfide concentrations for tracking reservoir souring processes and subsequent intervention effectiveness. Our results show that all three chemicals were effective at suppressing sulfidogenesis. A reactive transport model for perchlorate treatment was developed to simulate the reaction processes and explore the interactions between the underlying competing mechanisms of this inhibitor. A baseline simulation captured the temporal patterns of the effluent chemical species. Subsequent simulations in which individual inhibition mechanisms were systematically removed elucidated the relative role that each inhibition mechanism played at the different phases of the experiment. The simulation results complement the experimental findings. Our study supports the potential advantages of souring control with (per)chlorate treatments, and the application of galvanic signal as an economic, in-situ monitoring approach for tracking souring dynamics and treatment efficacy.

1. Introduction

Microbial souring in oil reservoirs, i.e. the production of hydrogen sulfide (H_2S) (via sulfidogenesis) due to the metabolism of sulfate reducing microbes (SRMs), is commonly encountered during the secondary recovery phase when sea water flooding is applied (Gieg et al., 2011). Hydrogen sulfide is a corrosive and highly toxic gas that poses serious threats to oilfield infrastructure, pipelines, and environmental and human health (Beauchamp et al., 1984; Reiffenstein et al., 1992). Measures and interventions associated with these threats cost the oil industry billions of dollars every year (Gregoire et al., 2014).

Currently, the main strategies for reservoir souring control include sulfate removal from the injection water, H_2S scavenging, reservoir biocide treatment and thermodynamic controls (Gieg et al., 2011). Amongst these different approaches, thermodynamic control methods are gaining popularity (Engelbrektson et al., 2014; Gregoire et al., 2014; Hubert and Voordouw, 2007). Such methods work with the principles of reaction thermodynamics by injecting energetically more favorable electron acceptors, such as nitrate, into soured reservoirs (Voordouw et al., 2009; Hubert, 2010; Hubert and Voordouw, 2007). Since nitrate reduction is energetically more favorable than sulfate reduction, it tends to occur first, outcompeting sulfate reduction for

* Corresponding author.
E-mail address: YWu3@lbl.gov (Y. Wu).
[1] Now at Cardiff University, UK.

https://doi.org/10.1016/j.chemgeo.2017.11.016
Received 15 May 2017; Received in revised form 6 November 2017; Accepted 14 November 2017
Available online 17 November 2017

limited electron donors (also known as bio-competitive exclusion). In addition, studies have found direct inhibitory/toxicity effects of nitrite (an intermediate during nitrate reduction) on microbial sulfate reduction (Callbeck et al., 2013). Nitrate addition can also stimulate nitrate reducing, sulfide oxidizing bacteria (NR-SOB) that can remove sulfide by coupling nitrate reduction to sulfide oxidation (De Gusseme et al., 2009; Hubert and Voordouw, 2007). While nitrate treatment is the prevailing souring control option, chlorate and perchlorate, collectively (per)chlorate, have recently been investigated as new candidate inhibitors.

Similar to nitrate, (per)chlorate reduction is also energetically more favorable than sulfate reduction. Earlier studies have also pointed to specific inhibitory/toxicity effects of (per)chlorate on sulfate reduction (Baeuerle and Huttner, 1986; Carlson et al., 2014; He et al., 2010; Postgate, 1952; Sunde and Torsvik, 2005). In addition, dissimilatory (per)chlorate reducing microbes (DPRM) innately oxidize H_2S to non-soluble elemental sulfur (Coates and Achenbach, 2004; Coates et al., 1999; Mehta-Kolte et al., 2017), thus removing the source of souring from the fluid phase irreversibly. As such, (per)chlorate has been suggested and tested as an alternative, and potentially more effective sulfide inhibitor (Engelbrektson et al., 2014; Gregoire et al., 2014). However, because the microbes that can readily metabolize (per)chlorate are not naturally abundant due to the scarcity of (per)chlorate in nature, how (per)chlorate addition stimulates DPRMs growth and functionality toward sulfate inhibition is still under investigation. In addition, how the (per)chlorate toxicity effect, bio-competitive exclusion effect, and its direct sulfide oxidation effect work in concert to achieve the overall suppression of sulfate reduction requires further investigation.

In addition to understanding the mechanisms controlling the effectiveness of each inhibitor in suppressing sulfide production in oil reservoirs, effective and economic methods to monitor H_2S concentration are also critical for tracking the progression of biosouring and the evaluation of the efficacy of any interventions. Currently, such evaluations are carried out based on the measurements of H_2S concentrations in the production fluids (often the gas phase) at the ground level, e.g. using the Draeger tube method. These methods provide only discrete measurements that often lack accuracy due to sulfide loss from pressure change or volatilization during sample handling. In addition, such methods often require handling of fluids with extreme precaution due to the toxicity of the sulfide gas even at very low concentrations (Reiffenstein et al., 1992). The importance of monitoring sulfide evolution during souring and its intervention calls for safe and economic downhole monitoring strategies capable of measuring sulfide concentrations in the reservoir under the in situ pressure and temperature conditions, without human exposure, in real time, continuously, and at low cost. Downhole in situ measurements also allow sulfide monitoring in injection or production wells during the idle periods when no fluid samples are available for direct measurements.

Electrochemical methods offer the potential to meet these challenging monitoring objectives. It is well recognized that redox active ions, sulfide in this case, can be detected using electrochemical methods based on redox (i.e. galvanic) reactions occurring between a measurement electrode situated in the sulfide monitoring zone and a reference electrode outside of the monitoring zone due to the presence of a redox gradient between these two electrodes that drives half cell reactions. Metals including platinum, silver, copper and gold amalgam alloy are amongst the materials that have been studied for sulfide detection and the sensitivity of these electrodes has been tested in the laboratory and some field studies (Brendel and Luther, 1995; Kapusta et al., 1983; Personna et al., 2008; Williams et al., 2007; Williams et al., 2010; Zhang et al., 2010). For example, Williams et al. (2007, 2010), Personna et al. (2008) and Zhang et al. (2010) conducted experiments on microbial sulfate reduction and found a correlation between sulfide occurrence and a decrease of the electrodic potential of Ag/AgCl and $Cu/CuSO_4$ electrodes. Kapusta et al. (1983) studied the effect of sulfide oxidation on platinum electrode surface and associated electrochemical signals. Brendel and Luther (1995) demonstrated the sensitivity of gold amalgam alloy electrodes to dissolved sulfide (along with several other redox sensitive species) in aqueous solutions using voltammetric methods. While the sensitivity of galvanic signal to the presence of sulfide has been demonstrated, studies on the accuracy of galvanic measurements in providing quantitative estimation of sulfide concentration have been limited, particularly for systems undergoing complex biogeochemical treatments in complex aqueous geochemical conditions commonly encountered in the oilfield reservoirs.

The objectives of this study were to (1) evaluate the relative efficacy of souring interventions through the injection of nitrate, chlorate and perchlorate solutions and explore the different mechanisms (i.e. toxicity, bio-competitive exclusion, direct sulfide oxidation) contributing to their inhibition effects on sulfidogenesis, (2) investigate the specific mechanisms underlying the effectiveness of the perchlorate treatment via reactive transport modeling of the system, and (3) explore the feasibility of galvanic potential measurements for rapid and quantitative monitoring of souring and desouring processes. Microbes from the San Francisco bay water were incubated and used to induce the souring conditions in the laboratory experiments, similar to the microbial community introduced into offshore oil reservoirs during the secondary recovery with seawater injection.

2. Materials and methods

2.1. Column experiments

Two sets of column experiments with different mineral matrices and inoculation strategies were conducted in order to assess the impacts of solid matrix and treatment procedures on souring development, souring treatments efficiency and the associated galvanic potential signals. Four columns were set up in each set of experiments (sandstone and bay mud); eight columns were set up in total. Each column received one type of treatment that included nitrate, chlorate, perchlorate and control (no treatment) (Fig. 1). The bay mud and sandstone columns were ran for ~20, and 50 days, respectively. All experiments were conducted under room temperature (20 ± 2 °C), and ambient pressure conditions with additional 1–2 PSI nitrogen (N_2) head space pressure at the influent bottles.

Both unconsolidated and consolidated matrices were evaluated. The unconsolidated column experiments were conducted using pre-soured Ottawa sand and San Francisco bay mud mixture packed in transparent PVC columns (3″ ID × 7″ length, hereafter referred to as bay mud columns). While not measured, due to the unconsolidated nature of the material, the expected permeability of the packed column was in the range of a few Darcies. The bay mud/bay water matrix served as the source of the microbial community, including sulfate reducers, indigenous to the marine environment (bay water/mud and microbial inoculum obtained from Engelbrektson and Coates lab at UC Berkeley). The bay mud and bay water mixture was incubated and pre-soured with 2 g/L yeast extract under anaerobic and ambient temperature conditions for several days to enrich the microbes before packed into the columns.

A second set of column experiments was conducted with Berea sandstone cores (Cleveland Quarries, 1.5″ ID × 4″ length, hereafter referred to as sandstone columns) cast with epoxy resin in PVC columns. Berea is a well-characterized quarried sandstone used for reservoir petrophysics studies. The purpose of the epoxy casting was to eliminate wall effects on laminar flow in the columns (Cohen and Metzner, 1981). The sandstone cores were sterilized at 120 °C for 2 h before the experiment. The permeability of the sandstone cores is ~100 milliDarcy as measured by gas permeametry, at least an order of magnitude smaller than that of the bay mud columns. Four columns were also setup for this experiment: one as the control column that was soured but received no desouring treatments and three other columns

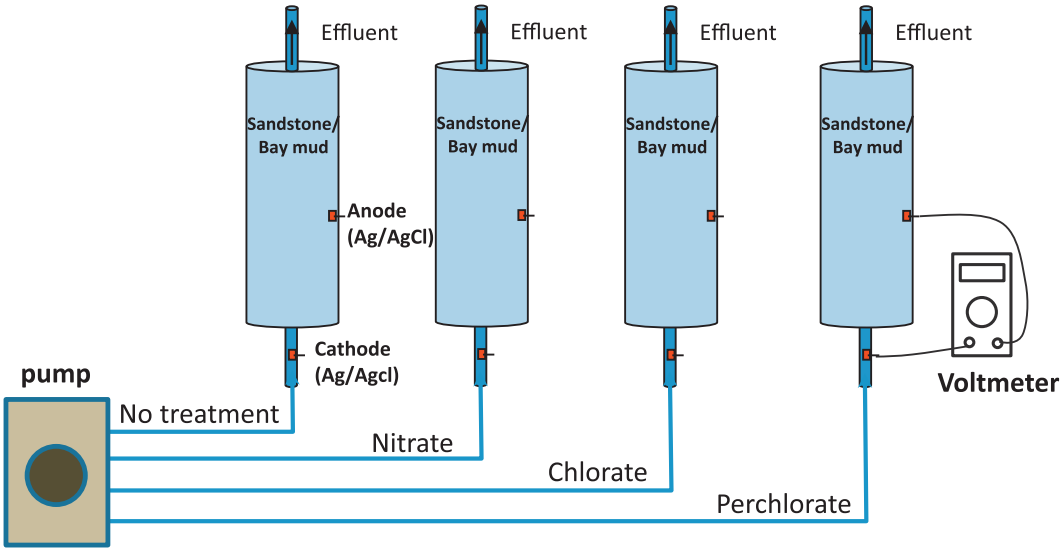

Fig. 1. The experiment setup for the biosouring and desouring treatments. Four columns were setup for each experiment with one control (no treatment) column and one for each of the treatments with nitrate, chlorate and perchlorate. Ag/AgCl electrodes were used as the cathode and anode electrodes for galvanic monitoring. The galvanic potentials were measured with a voltmeter.

treated with nitrate, chlorate and perchlorate, respectively, after the initial souring conditions had been established. Microbes enriched from San Francisco Bay mud were used to inoculate the sandstone columns in order to achieve similar initial microbial community condition with the bay mud columns.

For both sets of columns, water obtained from San Francisco Bay was used as the saturating media as well as the carrier fluid for nutrients and treatments throughout the experiments. The selection of bay water was made to simulate secondary recovery with seawater flooding and to evaluate the effects of high salinity and complex water chemistry on the souring process, the effectiveness of the treatments, and on the measured galvanic signals. 2 g/L yeast extract was added to the bay water as the nutrient source and 50–60 mM nitrate, chlorate and perchlorate solutions were injected into the three different treatment columns respectively during the desouring phase. All solutions were autoclaved at ~120 °C for 1 h and kept under nitrogen headspace (1–2 psi) throughout the experiments to maintain an anaerobic environment similar to the conditions in the oil reservoirs. The flow rates were regulated with peristaltic pumps and maintained at ~2 pore volumes per day for both sets of columns throughout the experiments. Desouring treatments in both sets of columns were started once significant amounts of sulfide were measured in the column effluents with colorimetric methods (Cline, 1969; Cord-Ruwisch, 1985). For these colorimetric methods, chemical reagents, including *N*, *N*-dimethyl-*p*-phenylenediamine sulfate, ferric chloride, copper sulfate and hydrochloric acid were used to develop colors with intensity proportional to sulfide concentration before measurements with spectrometers at 480 or 670 nm wavelengths. Other key effluent geochemistry parameters (sulfate, nitrate, chlorate and perchlorate) were measured with Ion Chromatography (Dionex).

Ag/AgCl electrodes were used to measure the galvanic signals from both sets of columns. The reference electrodes were installed on the upstream influent tubing separated from the columns in order to avoid sulfide contamination, thus providing a stable reference (Fig. 1). The measurement electrodes were installed in the middle of the columns, penetrating ~1 cm into the mineral matrices. The measurements were made based on the galvanic reactions between the reference electrodes and the measurement electrodes when bridged by a high impedance voltmeter (Fluke). The half cell and overall reactions of the galvanic cell are given below (Williams et al., 2007):

$$\text{Cathode}\quad AgCl_{(s)} + 1e^- \rightarrow Ag^0_{(s)} + Cl^-_{(aq)} \quad E^0_{half} = 0.22\ \text{V} \tag{1}$$

$$\text{Anode}\quad Ag_2S_{(s)} + H^+ + 2e^- \rightarrow 2Ag^0_{(s)} + HS^-_{(aq)} \quad E^0_{half} = -0.27\ \text{V} \tag{2}$$

$$\text{Overall}\quad 2AgCl_{(s)} + HS^-_{(aq)} \rightarrow Ag_sS_{(s)} + H^+ + 2Cl^-_{(aq)} \quad \Delta E_0 = 0.49\ \text{V} \tag{3}$$

The reference electrode serves as the cathode that undergoes reductive reaction ($Ag^+ \rightarrow Ag^0$) while the measurement electrodes acts as the anode that undergoes oxidation ($Ag^0 \rightarrow Ag^+$); the potential difference between the two electrodes can be calculated based on the Nernst equation (Stock and Orna, 1989):

$$\Delta E = \Delta E^0 - \frac{0.0592\ \text{V}}{n} \log \frac{[H^+][Cl^-]^2}{[HS^-]} \tag{4}$$

where ΔE is the measured galvanic potential, ΔE^0 is the standard galvanic potential (here, $\Delta E^0 = 0.49$ V) when the concentrations of the ions involved in the reactions are at 1 M, and n (here, $n = 2$) is the number of electrons transferred when one HS^- molecule is reacted. The Nernst equation predicts a logarithmic correlation between sulfide concentration and galvanic potential, which provides the basis for sulfide quantification with galvanic potential measurements.

2.2. Reactive transport modeling

A multicomponent reactive transport simulator, CrunchTope (Steefel and Maher, 2009; Druhan et al., 2012; Druhan et al., 2013; Druhan et al., 2014), was used to model the biogeochemical and flow processes in the perchlorate treated columns. In this study, we focused on perchlorate as experimental and modeling studies on its efficacy as souring treatment are relatively fewer (Engelbrektson et al., 2014; Cheng et al., 2016; Mehta-Kolte et al., 2017) than that of nitrate. A general reactive transport equation for chemical species, I, is represented as:

$$\frac{\partial(\phi S_L C_i)}{\partial t} = \nabla\cdot(\phi S_L D_i \nabla C_i) - \nabla\cdot(qC_i) - \sum_{j=1}^{Nj} v_{ij} R_j - \sum_{g=1}^{Ng} v_{ig} Rg - \sum_{m=1}^{Nm} v_{im} R_m \tag{5}$$

where, the term on the left hand side is the accumulation term and the terms on the right hand side are diffusion, advection and reaction terms (R_j: aqueous phase reactions, R_g: gas reactions, R_m: mineral reactions), respectively. ϕ is porosity, S_L is liquid saturation, C_i is concentration (mol kg^{-1}_{water}), D is the diffusion coefficient ($m^2\ s^{-1}$) and q is the Darcy flux ($m\ s^{-1}$) (Steefel et al., 2014; Druhan et al., 2014).

Table 1
Microbial reactions modeled. Values of *fs* and *fe* are determined by the types of electron donors and acceptors involved in the reaction using free energy values as described in Rittman and MaCarty (2001).

	Microbial reactions
1	Sulfate reduction ($SO_4^{2-} \rightarrow H_2S_{(aq)}$) (*fs* = 0.08, *fe* = 0.92) $0.115SO_4^{2-} + 0.125DOC + 0.004NH_3 + 0.23H_2O + 0.01H^+ \rightarrow 0.004C_5H_7O_2N_{SRB} + 0.23HCO_3^- + 0.115HS^-$
2	Heterotrophic perchlorate reduction ($ClO_4^{2-} \rightarrow Cl^-$) (*fs* = 0.45, *fe* = 0.55) $0.05625ClO_4^{2-} + 0.125DOC + 0.0275NH_4^+ + 0.0525H_2O \rightarrow 0.0275C_5H_7O_2N_{PRB} + 0.2475HCO_3^- + 0.05625Cl^- + 0.2475H^+$
3	Perchlorate reduction sulfide oxidation ($HS^- \rightarrow S_{(aq)}$) (*fs* = 0.0, *fe* = 1.0) $0.125ClO_4^- + 0.5H^+ + 0.5HS^- \rightarrow 0.125Cl^- + 0.5H_2O + 0.5S_{(aq)}$

Microorganisms (MB) mediate the reaction between an electron donor and an electron acceptor (i.e. sulfate and perchlorate in this study) to derive energy for growth and maintenance. The conceptual approach as described in Rittman and MaCarty (2001) has been adopted in CrunchTope to relate bacterial growth and energetics. Microbially mediated reactions are divided into two main components: catabolic and anabolic. For each mole of electron donor/substrate oxidized, a fraction, *fe*, is used for energy production (catabolic). The remaining fraction, *fs* (where *fs* + *fe* = 1), is conserved by the microbial biomass for cell synthesis (anabolic). The main reactions involving sulfate and perchlorate reduction are showing in Table 1 below. Readers are referred to Rittman and MaCarty (2001) for detailed derivation of the stoichiometric equations. Rates of microbially mediated reactions are described as follows:

$$r = \mu[\mathrm{MB}]K_T \tag{6}$$

where, r (mol kg_{water}^{-1} day^{-1}) is rate of the reaction as mediated by MB (represented as $C_5H_7O_2N$), μ (mol $mol_{C5H7O2N}^{-1}$ day^{-1}) is the maximum specific utilization rate. Kinetic constraints on the reaction rate by electron acceptors/donors and inhibitors are mathematically represented as:

$$K_T = \frac{[\mathrm{eDonor}]}{[\mathrm{eDonor}] + K_{\mathrm{eDonor}}} \frac{[\mathrm{eAcceptor}]}{[\mathrm{eAcceptor}] + K_{\mathrm{eAcceptor}}} \frac{K_{\mathrm{Inhibitor}}}{[\mathrm{Inhibitor}] + K_{\mathrm{Inhibitor}}} \tag{7}$$

$K_{\mathrm{eDonor/eAcceptor}}$ (mol kg_{water}^{-1}) is the half saturation (affinity constant) of the electron donor/acceptor, while $K_{\mathrm{Inhibitor}}$ (mol kg_{water}^{-1}) is the inhibition constant.

The kinetic parameters of the reactions in Table 1 are listed below in Table 2.

The inhibition constants of the reactions in Table 1 are shown in Table 3.

2.3. Model setup and simulations

A reactive transport model of the sandstone column was developed. The simulation domain consisted of 100 nodes; each with a resolution of 0.001 m (1 mm). Porosity was set at 0.15. A constant flow velocity of two pore volumes day^{-1} was prescribed based on the experimental condition.

Table 2
Kinetic parameters of reactions in Table 1.

Microbial reactions (from Table 1)	μ (mol mol-cell^{-1} day^{-1})	$K_{acceptor}$ (mol kg_{water}^{-1})	K_{donor} (mol kg_{water}^{-1})
1	264[a]	5.0×10^{-4}[b]	1.0×10^{-3}[c]
2	132	1.0×10^{-2}	1.0×10^{-2}
3	176	5.0×10^{-3}	5.0×10^{-3}

[a] Druhan et al. (2012, 2014), Jin and Roden (2011), Cheng et al. (2016).
[b] Pallud and Van Cappellen (2006), Porter et al. (2007), Fang et al. (2009), Li et al. (2009), Jin and Roden (2011), Druhan et al. (2012, 2014), Cheng et al. (2016).
[c] Pallud and Van Cappellen (2006), Porter et al. (2007), Fang et al. (2009), Li et al. (2009), Jin and Roden (2011), Druhan et al. (2012, 2014), Cheng et al. (2016).

Table 3
Inhibition constants of reactions in Table 1 and decay constants of microorganisms.

Microbial reactions (from Table 1)	Inhibitor	K_{inhib} (mol kg_{water}^{-1})
2	Perchlorate	1.5×10^{-3}[a]
3	Sulfide	2.0×10^{-3}
Microorganism	Decay constant (day^{-1})	
Sulfate reducing microorganism	2.0×10^{-2}[b]	
Perchlorate reducing microorganism	2.0×10^{-2}	

[a] Range: 2.0×10^{-3}–30.0×10^{-3} M based on Carlson et al. (2014).
[b] Range: 2.0×10^{-3}–2.0×10^{-2} Yabusaki et al. (2011), Druhan et al. (2012, 2014), Cheng et al. (2016).

As discussed above, known mechanisms by which perchlorate inhibits sulfide production include: (1) direct toxicity/inhibitory effects on SRM activities by perchlorate (Postgate, 1952; Baeuerle and Huttner, 1986; Carlson et al., 2014), (2) indirect inhibition of the SRM through competition for electron donors from DPRM (Engelbrektson et al., 2014), and (3) perchlorate reducing sulfide oxidizing (PRSO) activity of the DPRM (Mehta-Kolte et al., 2017), oxidizing sulfide to elemental sulfur. Mehta-Kolte et al. (2017) showed that perchlorate reducers mediate both heterotrophic perchlorate reduction and perchlorate reduction linked to sulfide oxidation (reactions 2 & 3 in Tables 1) in batch culture experiments. However, the latter mechanism is preferred and no growth is observed in association with this mechanism. On the other hand, perchlorate reducers grow during heterotrophic perchlorate reduction, a pathway that is inhibited in the presence of sulfide. To model this, we used the same DPRM population to mediate both pathways, with a sulfide inhibition constant applied to heterotrophic perchlorate reduction (Table 3).

Yeast extract (2 g/L) is used as an electron donor in the experiment. A simple anaerobic bottle experiment with San Francisco Bay water, sediment and yeast extract showed that 1 g/L yeast extract reduced 18.2 mM sulfate, equivalent to ~20 mM of acetate according to our reaction stoichiometry (Table 1). Therefore in our simulation, 2 g/L of yeast extract is represented by 40 mM acetate. Next, we need to constrain the amount of NH_4 to represent in the simulations. Yeast extract typically contains 10–11 wt% N. For 1 g/L yeast extract, this is equivalent to 7.5 mM N. Therefore, 15 mM NH_4 is used in our simulations.

Once established, the reactive transport models were used to explore the importance of different microbial-mediated pathways under varying geochemical conditions. The following scenarios were explored to isolate the effect of different inhibition mechanisms to sulfide production: (a) All mechanisms included (Table 1, reactions 1–3), (b) direct toxicity/inhibition effects from perchlorate on sulfate reduction excluded, (c) heterotrophic perchlorate reduction excluded (excluding reaction 2 in Table 1), and (d) perchlorate reduction, sulfide oxidation excluded (reaction 3 in Table 1). These simulation results were compared with the geochemical data from the experiments to understand their relative contribution/importance to the overall reaction processes over time.

3. Results

3.1. Sulfide and galvanic potential

Microbial sulfate reduction as the initial condition/phase of the experiments was successfully stimulated in both sets of columns. The evolution of sulfide concentrations from the effluents and the galvanic potentials measured in the middle of the columns for the bay mud

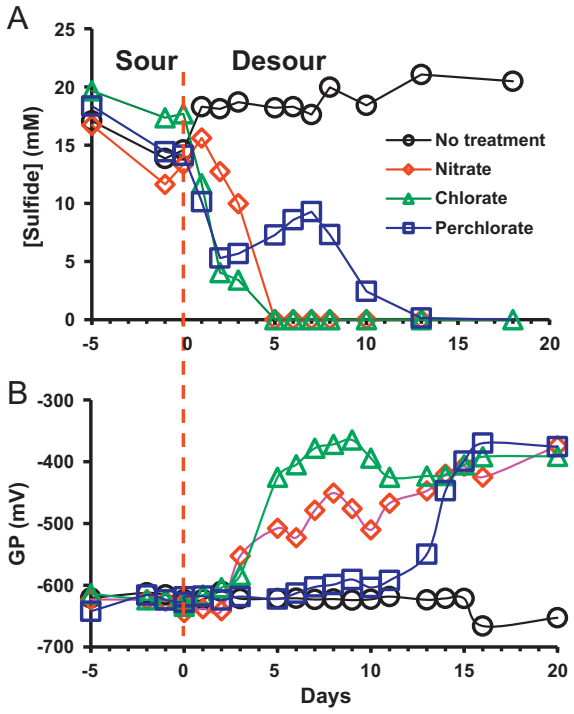

Fig. 2. (A) Effluent sulfide concentration and (B) galvanic potential (GP) measurements over time in the bay mud columns. Control column (black) is compared to three treatment columns, nitrate (red), chlorate (green), and perchlorate (blue). Day 0 represents the starting of the desouring treatments. The red dashed line separate the first (sour) and second (desouring) phase of the experiment. (For interpretation of the references to color in this figure legend, the reader is referred to the web version of this article.)

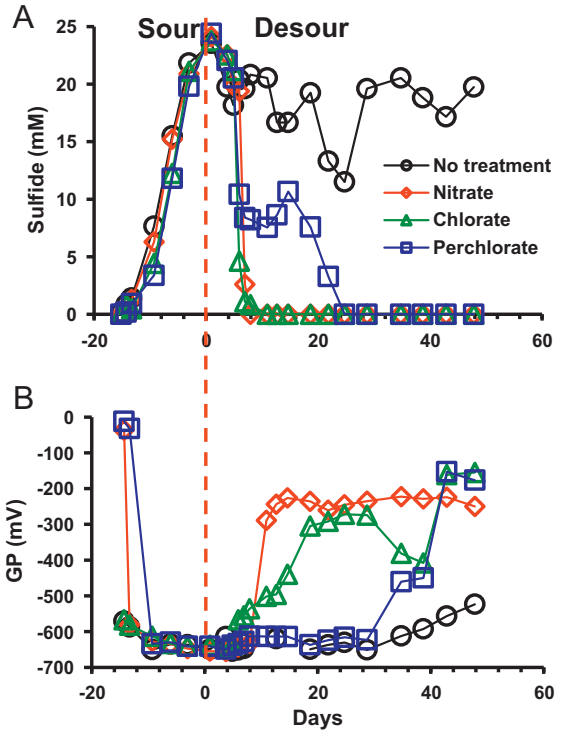

Fig. 3. (A) Effluent sulfide concentration and (B) galvanic potential (GP) measurements over time in the sandstone columns. Control column (black) is compared to three treatment columns, nitrate (red), chlorate (green), and perchlorate (blue). Day 0 represents the starting of the desouring treatments. The red dashed line separate the first (sour) and second (desouring) phase of the experiment. (For interpretation of the references to color in this figure legend, the reader is referred to the web version of this article.)

columns are shown in Fig. 2. The Ottawa sand and bay mud mixture was pre-soured before being packed into the columns and our data showed sulfide concentrations ranging from 12 to 20 mM at the beginning of the experiments (the sour phase) (Fig. 2A), indicating sustained, significant microbial sulfate reduction in the bay mud columns during seawater injection. Concurrently, galvanic potential measurements showed a strong signal at ~ − 630 mV (Fig. 2B) during this initial souring phase, indicating a strong reducing condition in the columns due to the production of sulfide. During the second phase, desouring treatments with nitrate, chlorate and perchlorate were successful, indicated by the decrease in effluent sulfide concentrations in all three treatment columns, while sulfide concentrations in the control (no treatment) column sustained at ~20 mM throughout the experiments (Fig. 2A).

In contrast to the bay mud columns that were pre-soured before the experiment started, microbial inoculation and subsequent sulfidogenesis occurred after column setup and flow establishment in the sandstone columns. Galvanic monitoring of the sandstone columns started before microbial inoculation. Sulfide concentrations measurements started immediately after the microbial inoculation at day − 13 (day 0 being the start of the desouring treatments) and showed an increase from 0 to ~24 mM at the effluent within ~14 days (Fig. 3A). Accompanying microbial sulfate reduction was a steep decrease of galvanic potential measurements from ~0 mV to ~ − 650 mV (Fig. 3B), indicating a strong decrease of the redox potentials similar to the observation from the bay mud columns. Desouring treatments in the sandstone columns were similarly successful when compared to the bay mud columns, showing decreases of sulfide concentrations to below detection limits over time.

During the desouring treatments of the bay mud columns, while the galvanic potential measurements in the control columns stayed stable at ~ − 630 mV, the measurements in the treated columns increased to ~ − 400 mV, in responding to the decrease in sulfide concentrations (Fig. 2B). We note two additional features of the galvanic potential response from Fig. 2: (a) galvanic response lagged sulfide concentration changes by ~2 days, and (b) a remnant galvanic potential of ~ − 400 mV still existed at the end of the experiment for all three treated columns. Galvanic responses from the desouring treatment of the sandstone columns were very similar to the bay mud columns, showing an increase over time with a lagged response by a few days and a remnant value at ~ − 200 mV to − 300 mV at the end of the experiments (Fig. 3B).

It is important to note that while continuous and rapid decrease of sulfide concentrations were observed for both sets of the experiments treated with nitrate and chlorate, the perchlorate treated columns showed a distinct phased and delayed response (Figs. 2A, 3A). Specifically, the sulfide concentrations in the perchlorate treated columns initially dropped approximately by 70%, then followed by a few days of rebound by ~5 mM before further decreasing to below the detection limit. This was observed for both the bay mud and the sandstone columns regardless of their differences in matrix properties, hydraulic conditions and microbial inoculation strategies. This provides insights on the different sulfidogenesis inhibition mechanisms from perchlorate treatments, which will be discussed later.

3.2. Effluent sulfate and inhibitors

In addition to sulfide and galvanic potential measurements, effluent sulfate and chemical inhibitor concentrations (i.e. nitrate, chlorate and perchlorate) were also monitored in both sets of columns in order to better explore the different biogeochemical mechanisms driving sulfidogenesis and inhibition for different treatments.

The dynamic change of the effluent sulfate concentrations with time revealed distinct differences between the different treatments in the bay mud columns (Fig. 4A). The control column showed low sulfate

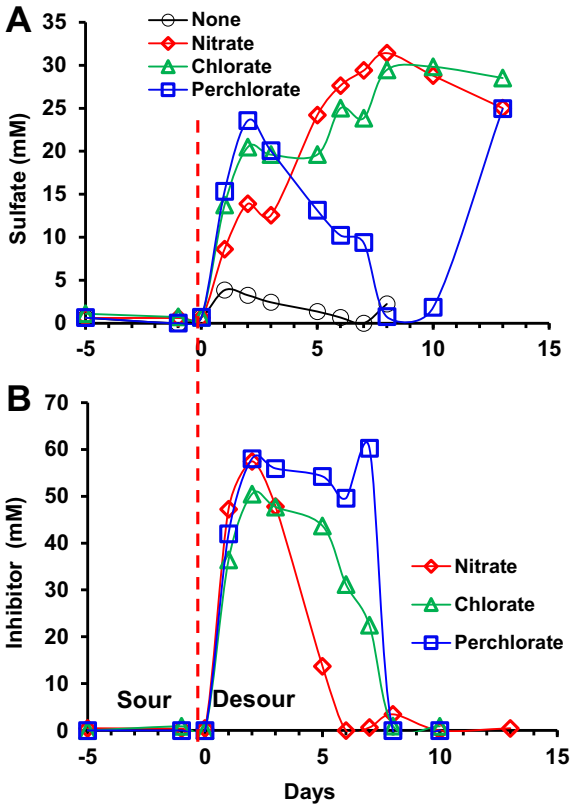

Fig. 4. The evolution of effluent (A) sulfate and (B) chemical inhibitor concentrations in the bay mud columns during the experiments. Day 0 represents the starting of the desouring treatments.

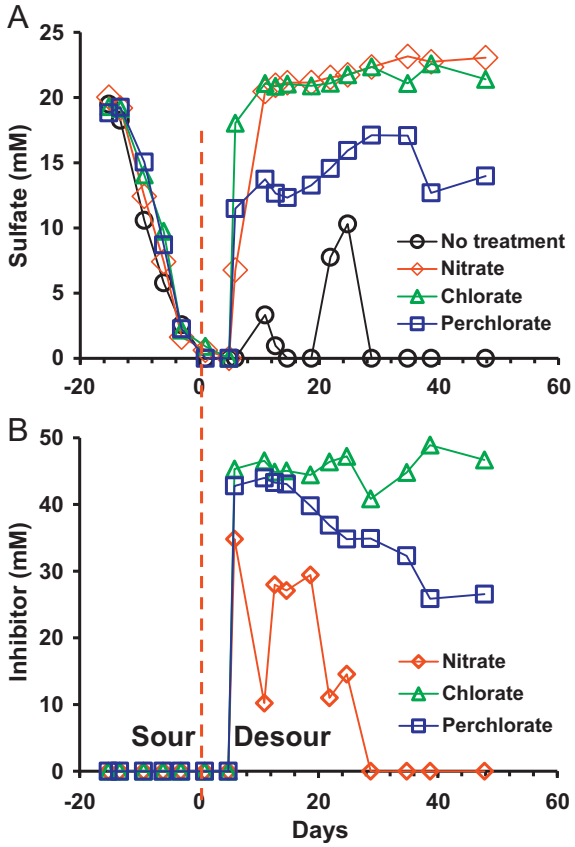

Fig. 5. The evolution of effluent (A) sulfate and (B) chemical inhibitor concentrations in the sandstone columns during the experiments. Day 0 represents the starting of the desouring treatments.

concentrations (< 5 mM) throughout the experiments due to sustained sulfidogenesis. Upon beginning the desouring treatments at day 0, the nitrate treated columns showed a near continuous increase in sulfate concentration until they stabilized at the end of the experiment. The chlorate treated column showed a stepped increase in sulfate concentrations which plateaued (day 2–5) after an initial sharp increase, and were followed by an additional increase before concentrations stabilized at near influent values. Unlike nitrate and chlorate, sulfate concentrations in the perchlorate treated column showed a very different behavior. Specifically, an initial sharp increase was observed from day 0–2, similar to nitrate and chlorate columns, but were followed by a period of graduate decrease to almost complete disappearance from day 2–8 before further increasing to concentrations comparable to the nitrate and chlorate treated columns at the end of the experiments. Note that the decrease of effluent sulfate concentrations in the perchlorate treated column from day 2–8 coincided with the increase of sulfide concentrations (Fig. 2A) while their magnitudes were different (i.e. > 20 mM sulfate decrease vs. 5 mM sulfide increase), indicating a loss of total sulfur mass from the aqueous phase.

Effluent inhibitor concentrations provided an additional important dataset for exploring sulfidogenesis inhibition mechanisms during the different treatments (Fig. 4B). After an initial sharp increase of the inhibitor concentrations following the starting of the flow (day 0–2), sharp decrease of effluent concentrations over the next 4–6 days was only observed for nitrate until their near complete utilization for the rest of the treatments. While a continued decreasing trend for chlorate is shown, chlorate consumption was sustained at a relatively slow rate from day 2–5 before a sharp increase. Similar to chlorate, the perchlorate concentrations stayed at relatively high level with only slight decrease before a sharp decrease to below the detection level. Note that the nitrate consumption rates reached the maximal level earlier than both chlorate and perchlorate.

Effluent sulfate and chemical inhibitor concentrations in the sandstone columns showed similar behavior for nitrate column, yet different for chlorate and perchlorate columns when compared with the bay mud columns (Fig. 5). Specifically, the effluent concentrations of chlorate and perchlorate were sustained at > 50% influent level throughout the experiments, particularly for chlorate where only minor consumption was evident for a short period. Although the experiment was conducted for a much longer time (~50 days), the chlorate/perchlorate behavior is similar to the initial phase of the bay mud columns (day 2–8). The sandstone columns did not progress into total consumption of chlorate and perchlorate even at the end of the experiment, contrasting to the observations from the bay mud columns.

Despite the minimal consumption of chlorate and perchlorate, sulfate reduction appeared to be suppressed in the sandstone columns, supported by the rebound of sulfate concentrations (Fig. 5A) and the disappearance of sulfide from the effluents (Fig. 3A). Note that the sulfate concentration in the perchlorate treated column never rebounded to the influent level at the end of the experiment despite the complete disappearance of sulfide.

3.3. Model simulations

In the perchlorate treated sandstone column, the model reproduced the observed trends of effluent sulfate, sulfide, and perchlorate data (blue lines, Fig. 6). Data showed that perchlorate breakthrough and effluent concentration increased rapidly within 5 days to influent concentration values, before gradually decreasing to around 27 mM for the period at the end of the experiment (Fig. 6a). The initial breakthrough of perchlorate was accompanied by rapid decrease of sulfide concentrations to ~8 mM, followed by a rebound to ~11 mM before rapidly dropping to 0 mM around day 24 (Fig. 6b). Thereafter, effluent

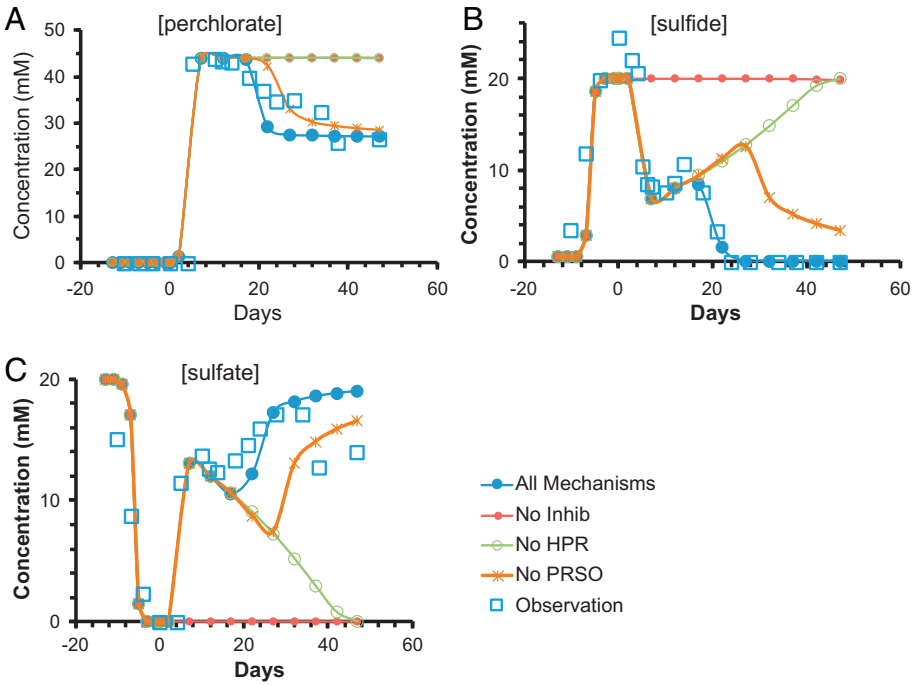

Fig. 6. Observed (blue squares) and simulated (blue, red, green and orange lines) effluent (a) perchlorate, (b) sulfide and (c) sulfate from the sandstone column experiments. The blue lines represent simulation results for the case in which all inhibition mechanisms were represented. The red lines represent simulation results for the case in which the direct inhibition of perchlorate on sulfate reduction is excluded. The green lines represent simulation results for the case in which heterotrophic perchlorate reduction is excluded. (For interpretation of the references to color in this figure legend, the reader is referred to the web version of this article.)

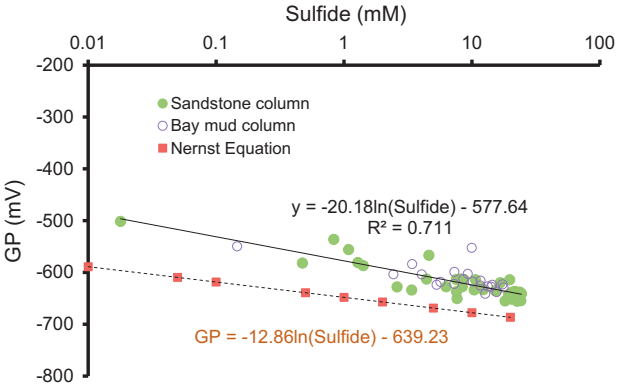

Fig. 7. Correlations between sulfide concentration and galvanic potential for both the bay mud and sandstone columns and its comparison with theoretical values based on the Nernst equation.

sulfide concentration remained undetectable till the end of the experiment. The behavior of effluent sulfate was inverse of that of the effluent sulfide. The initial breakthrough of perchlorate was accompanied by rapid increase of sulfate concentrations to 13.7 mM, followed by a short reduction period that corresponds to the rebound of the sulfide concentration. After the reduction period, effluent sulfate continued to increase to ~15 mM till the end of the experiment. Fig. 6 also showed simulation results excluding direct toxicity/inhabitation effects (No inhib, red line), heterotrophic perchlorate reduction (No HPR, green line) or perchlorate reduction sulfide oxidation (No PRSO, orange line) to explore the relative contribution from the different reaction pathways. The results demonstrated the relative impacts of the disparate processes on the effluent chemistry.

4. Discussion

The similarity and distinct differences between the system responses to the different treatments provided important dataset to explore the variable thermodynamic processes controlling sulfidogenesis inhabitation for the different treatments.

4.1. Sulfide and galvanic potential responses

Regardless of the differences in mineral matrix and inoculation conditions between the bay mud and sandstone columns, the sulfide concentrations evolved similarly in both sets of experiments in responding to the treatments with nitrate, chlorate or perchlorate. Namely, a quick decrease of sulfide concentrations to non-detectable level in nitrate and chlorate treated columns and a plateau followed by slight increase before further decrease for perchlorate treated columns.

Without considering the different inhibition mechanisms (to be discussed later), these datasets demonstrated the effectiveness and consistency of all three treatments under different physical and geochemical conditions (Figs. 2A, 3A). Similar to the sulfide evolution, the galvanic potential measurements also showed consistency between these two sets of experiments (Figs. 2B, 3B). In order to evaluate the efficacy of utilizing galvanic potential measurements for quantitative sulfide monitoring, the correlation between the galvanic potential measurements and the sulfide concentrations was analyzed combining datasets from both sets of columns (Fig. 7). For comparison, theoretically calculated galvanic potentials from the Nernst equation (Eq. (4)) were also shown based on the averaged geochemical parameters measured for the bay water used in the experiments (pH = 7.8, chloride concentration at ~485 mM).

A logarithmic correlation between the sulfide concentration and the galvanic potential measurement is apparent from Fig. 7 ($R^2 \sim 0.711$). This correlation is similar to the theoretical calculation based on the Nernst equation, but with a vertical shift of ~50 mV at high sulfide concentrations and a slight difference in slope. This discrepancy could result from a few possible reasons that include (a) the imperfection of the Ag/AgCl electrodes (i.e. deviation from the standard electrode potential) used in the experiments, (b) the aging and electrochemical changes of the electrodes during the experiment (e.g. anode electrode changing from Ag/AgCl to a Ag/AgCl/Ag_2S mix according to Eq. (2), altering surface exposure and ionic diffusion), (c) the variability and uncertainty in the measurements of pH, chloride and sulfide concentrations (particularly for sulfide due to its volatility leading to loss during sample handling), and (d) the discrepancy between where the sulfide concentrations were measured (effluent) and where the galvanic potential electrodes were positioned (middle of the columns). Despite

these caveats, the observed correlation between the sulfide concentrations and the galvanic potential measurements between these two sets of experiments under different conditions is similar to each other and close to the theoretical prediction, demonstrating the feasibility for quantifying sulfide concentrations based on simple and fast galvanic potential measurements.

The logarithmic correlation between the sulfide concentration and the galvanic potential shown in Fig. 7 points to the fact that changes in sulfide concentrations over a few orders of magnitude are readily resolvable through galvanic potential measurements, particularly during the onset of sulfate reduction, where a very small amount (e.g. submicromolar) of sulfide production can result in a large change of galvanic potentials from ~0 mV to a few hundred millivolts below zero. In fact, the remnant galvanic potential observed at the end of the experiments for both sets of columns (~− 200 mV and ~− 400 mV for bay mud and sandstone columns, respectively) could have resulted from very low concentrations of sulfide still present in the vicinity of the electrodes at the end of the experiments but were below the detection limits (0.001 mM for Cline assay and 0.1 mM for Cord-Ruwisch assay). Another possible reason for the remnant galvanic potential observed at the end of the experiments could be related to the electrochemical alterations of the anode electrodes imbedded in the middle of the column. Over time, Ag^0 dissolved with concurrent Ag_2S precipitation on the measurement electrodes, which could alter the potential of the anode electrodes irreversibly. Tests of these altered electrodes against unaltered Ag/AgCl electrodes in bay water after the experiments showed ~− 200 mV to − 300 mV differences in the electrode potentials, supporting this hypothesis. The irreversible alteration of the measurement electrodes in the monitoring process is a limitation of this particular technology for long-term field deployment, and an optimal monitoring approach will exhibit a fully reversible (or regenerable) response to capture variations in souring and desouring treatment response over a long deployment time.

We should also point out that the lag of the galvanic potential response to sulfide concentrations shown in Figs. 2 and 3 could possibly be related to the delayed changes of sulfide concentrations in the immediate vicinity of the measurement electrodes that were located close to the edge of the porous media. The timescale of this delay was likely related to the hydraulic properties (e.g. both overall and local permeability) of the solid matrix that affect solute transport, diffusion and reactions.

To assess the applicability of galvanic potential signals for in situ sulfide monitoring under oilfield reservoir conditions, the effects of elevated temperature and pressure conditions typical to hydrocarbon reservoirs need to be considered. While not tested, elevated temperature and pressure can affect galvanic potential by changing dissolved sulfide concentrations if excessive amount of sulfide is present and oversaturation is reached. The solubility of hydrogen sulfide decreases within increasing temperature, and at 60 °C and ambient pressure, the water solubility of hydrogen sulfide is ~44 mM, which is moderately higher than typical sulfate concentration in seawater (< 30 mM). This indicates that seawater is typically under-saturated with respect to sulfide even at 60 °C and assumes total conversion of sulfate to sulfide from microbial sulfate reduction. Therefore, temperature changes within a certain range (at least up to 60 °C) will not affect dissolved sulfide concentration directly. Similarly, we do not expect an effect from elevated pressure on sulfide concentration either in our study. However, while it is out of our scope, we note that elevated pressure and temperature conditions will likely affect microbial community composition and metabolic activity, which can subsequently affect sulfate reduction.

While our experiments demonstrate that the galvanic potential measurements can be used to monitor reservoir biogenic sulfide production and treatments under complex physical and geochemical conditions, additional developments are needed before it can be used for in-situ deployment in the oilfield reservoirs. These include the critical need to enhance the robustness/regenerability of the electrodes over a long monitoring period, and the design and integration of the galvanic monitoring system with existing oilfield wellbore infrastructure to allow downhole deployment and continuous and autonomous monitoring.

4.2. Sulfide inhibition mechanisms of nitrate treatment

In this experiment, nitrate treatment was effective at reducing sulfide concentrations to undetectable levels rapidly within a few days. Nitrate is known for effective stimulation of naturally abundant nitrate reducing bacteria that can outcompete sulfate reducers for electron donors (bio-competitive exclusion), making it attractive for souring control. In this work, the most rapid consumption of nitrate amongst the three treatments suggested the rapid response of the nitrate reducers to the stimulation and its immediate effectiveness in suppressing sulfidogenesis (Figs. 4B, 5B). Based on the mass conservation of the total sulfur species in the aqueous phase (i.e. the total mass of sulfate and sulfide), nitrate treatments appeared to have a pure bio-competitive exclusion effect in our experiments without noticeable effects from NR-SOBs that can directly oxide sulfide to elemental sulfur to cause a reduction of the total sulfur mass in the fluid phase. For bio-competitive exclusion to be effective enough mass of nitrate needs to be injected to exhaust the electron donors (e.g. acetate and VOCs in oil phase) in order to prevent their utilization by sulfate reducers. Engelbrektson et al. (2014) showed an increase in the sulfide concentration in nitrate treated columns after an initial period of inhibition, indicating unsustainable performance of nitrate as a sulfidogenesis inhibitor over the longer term following depletion of nitrate.

4.3. Sulfide inhibition mechanisms of (per)chlorate treatments – geochemical data

As discussed above, while nitrate treatment were effective at reducing sulfide concentrations to undetectable levels rapidly within a few days, a distinctly different response from (per)chlorate treatments were observed in both sets of experiments as shown in Figs. 2A and 3A. We explored the potential differences in the underlying mechanisms driving the responses of the system to (per)chlorate based on the geochemical data presented above.

Chlorate and perchlorate treatments resulted in different sulfide and sulfate responses when compared with nitrate. Data from the bay mud columns showed a larger initial suppression effect on sulfide concentrations in the first 2–3 days from chlorate and perchlorate treated columns when compared with nitrate column (Fig. 2A). This was accompanied by a concurrent larger rebound of the sulfate concentrations (Fig. 4A), indicating a large immediate effect of the chlorate and perchlorate treatments on sulfidogenesis. Similar patterns in effluent sulfide/sulfate concentrations were also observed by Engelbrektson et al. (2014). While microbial analysis were not conducted for this experiment, in Engelbrektson et al. (2014) where the same microbial inoculants with this experiments were used, analysis revealed dramatic differences in the microbial community shift between these different treatments. Specifically, chlorate and perchlorate treatments showed a suppressive/inhibitory effect on the microbial community when compared with the untreated controls, supported by a significant decrease in the abundance of SRMs. Engelbrektson et al. (2014) attributed this observation to the specific inhibitory/toxicity effects on SRMs by chlorate and perchlorate. In their study, Carlson et al. (2014) concluded that (per)chlorate act as direct inhibitors of the central sulfate-reduction pathway, and that (per)chlorate are more potent inhibitors than nitrate in both pure cultures and communities. This inhibitory/toxicity effect is likely the cause of the immediate suppression of sulfate reduction in chlorate and perchlorate treated columns at the beginning of the treatment. While the bio-competitive exclusion and sulfide oxidation may also be at work, they may not be as significant since in the

early stage, (per)chlorate reducing microbes were much lower in abundance in comparison to the SRMs, which were allowed to grow during the initial souring phase.

Following the initial toxicity effects, subsequent responses between the chlorate and perchlorate treated columns deviated from each other. This is best illustrated by the sulfate data in the bay mud columns (Fig. 4A). From day 2–8, the sulfate concentration in the chlorate treated column showed a short plateau before starting to increase again until reaching a stable concentration close to the influent concentration (~29 mM). The sulfate plateau was accompanied by concurrent and continued decrease of sulfide concentration (Fig. 2A), indicating a loss of the total sulfur mass from the aqueous phase. This suggests possible precipitation of non-soluble sulfur species, most likely elemental sulfur. Direct sulfide oxidation by DPRMs has been shown in previous studies (Coates and Achenbach, 2004; Coates et al., 1999; Gregoire et al., 2014). While no growth benefit for the microbes are known, recent studies have shown the preferential utilization of sulfide by certain DPRM strains as the electron donor over other physiological electron donors, such as acetate or lactate (Mehta-Kolte et al., 2017). Indeed, yellow precipitates (image not shown) were observed in the chlorate treated bay mud columns, which, although not analyzed in this study, was presumably elemental sulfur. Following this transitional period, sulfate concentration in chlorate column increased to a stable concentration close to the influent, suggesting a complete suppression of sulfidogenesis, likely due to combined effects of toxicity and bio-competitive exclusion of sulfate reduction.

Unlike the chlorate column that showed a stable or increasing sulfate concentration after treatment started, sulfate response in perchlorate treated column showed a continuous and significant decrease from day 2–8 (Fig. 4A), which is accompanied by a concurrent increase in sulfide concentration (Fig. 2A). A brief rebound of sulfidogenesis, indicated a possible weaker toxicity effect from perchlorate when compared with chlorate treatment. Carlson et al. (2014) showed chlorate is more inhibitory to sulfide production than perchlorate. In their study, the concentration at which chlorate inhibit 50% of sulfidogenesis (i.e. IC_{50}) is lower (1.6 mM) than that of perchlorate (2.3 mM). Note that, during this period the total sulfur mass in the aqueous phase showed a continuous decrease, pointing to direct sulfide oxidation from DPRMs (i.e. precipitation of elemental sulfur), similar to the observation from the chlorate column. After this transitional period, a quick rebound of the sulfate concentration was observed in the perchlorate treated column (Fig. 4A), accompanied by the concurrent decrease of sulfide concentration to below the detection limit. Taken together with the decrease in perchlorate concentration at around the same time (~day 8, Fig. 4B), these trends suggest that sulfidogenesis was also controlled by bio-competitive exclusion of sulfate reduction. Similar to Engelbrektson et al. (2014), while our geochemical data suggested the actions of three known inhibitory mechanism of (per)chlorate at work, it remained a challenge to elucidate the relative impacts of each mechanism.

4.4. Sulfide inhibition mechanisms of perchlorate treatment – reactive transport modeling

An integrated approach in which RTM simulation results were coupled to geochemical data to gain additional insights into the interactions between the underlying competing mechanisms of perchlorate was utilized. RTMs are processed based models that integrate disparate processes described by known mathematical formulations, allowing users to assess system response to environmental changes, or perform numerical experiments in times when data are not available (Li et al., 2017). The recent souring treatment experiment conducted by Engelbrektson et al. (2014) identified toxicity, sulfide oxidation and bio-competitive exclusion of sulfate reduction at work in perchlorate treatment. However, the experiment was not designed to elucidate the relative impacts of the inhibiting mechanisms. A follow up/companion RTM study of the Engelbrektson columns by Cheng et al. (2016) showed that bio-competitive exclusion of sulfate reduction was the most important mechanism in perchlorate treatment columns.

Comparison of the simulation results of the different cases showed the relative impact of each mechanism (direct inhibition, heterotrophic perchlorate reduction, PRSO) on effluent chemistry (Fig. 6). In the absence of direct inhibition of sulfate reduction by perchlorate (red lines in Fig. 6), sulfate reduction continued (after perchlorate injection at day 0) and effluent sulfate stayed at zero for the entire time of the experiment. Effluent sulfide remained high at ~20 mM (complete conversion of influent sulfate to sulfide). Effluent perchlorate remained close to influent values throughout the whole time. These results show that this inhibition mechanism plays a dominant role in the experiment.

In the absence of heterotrophic perchlorate reduction (green line in Fig. 6), the rate of perchlorate reduction becomes negligible, as shown by effluent perchlorate concentration matching influent values throughout the simulation timeframe. The direct inhibitory impact of perchlorate was only able to reduce sulfate reduction rates particularly in the first ~10 days. This mechanism was only responsible for reducing sulfide concentration to ~8 mM. Beyond day 10, sulfide concentration continued to increase to pre-treatment values at the end of the experiment, with corresponding decrease in sulfate concentration to zero.

Similar to the removal of heterotrophic perchlorate reduction, in the absence of PRSO (orange line in Fig. 6), an initial drop in effluent sulfide concentration with a concurrent rise in sulfate concentration was observed and can be attributed to the action of direct toxicity. The direct inhibitory impact of perchlorate was only able to reduce sulfate reduction rates particularly in the first ~10 days. Beyond day 10, sulfide concentration increased to ~12 mM at day 27, after which, sulfide concentrations dropped to as low as 3.5 mM at the end of the experiment. This drop, accompanied by the rise in sulfate concentration and also the reduction in perchlorate concentration suggested bio-competitive exclusion at work.

In all, these simulation results point to the toxicity impact of perchlorate as the most important mechanism for this set of perchlorate treatment columns. This is in contrast to the findings of Cheng et al. (2016) study, which showed bio-competitive exclusion to be the primary mode of mechanism for the Engelbrektson columns. However, it should be noted that in the Engelbrektson columns, the pre-souring phase was absent. During the pre-souring phase, the SRMs were allowed to grow uninhibited, increasing the sulfate reducing capacity of the system. The high sulfate reducing capacity in the soured system with limited electron donors and low abundance of perchlorate reducers translated to low perchlorate reducing capacity when perchlorate was first injected into the system.

In fact, Cheng et al. (2016) explored an additional scenario in which the perchlorate reducing capacity in the system is diminished with the SRMs being more sensitive to perchlorate toxicity (K_{inhib} = 2 mmol/kgwater, within known limits as shown in Carlson et al., 2014) than the original Engelbrektson perchlorate columns (K_{inhib} = 30 mmol/kgwater). This is similar to situations in soured oil reservoirs, where perchlorate reducers are not as naturally abundant as SRMs, and typically little is known about the perchlorate reducing capacity of the microbial population in the oil reservoir. The model scenario is also similar to the experimental setup in this study (in this study, K_{inhib} = 1.5 mmol/kgwater). Their simulation results also showed that perchlorate effectively suppressed SRM activity through toxicity as the main mode of action. Together results from both studies highlight: (1) the importance of the knowledge of site microbial community since it can impact the selection of perchlorate dose rates, and (2) the need for measurements of perchlorate inhibition constants of oil reservoir SRMs (pure cultures and communities) to improve future model predictions.

4.5. Cross columns comparison

The effluent geochemical results from the sandstone columns (Fig. 5) showed some deviation from those of the bay mud columns. Specifically, the initial breakthroughs of all three chemical inhibitors were accompanied by rapid decrease of sulfide concentrations, except the perchlorate column where a rebound was observed, similar to the bay mud columns. For both nitrate and chlorate columns, sulfide concentrations decreased to below detection level by day 5 and sustained at this level until the end of the experiment. This is accompanied by the rebound of sulfate concentrations to ~20 mM, also sustained for the rest of the experiments. During this period, nitrate concentration continued to decrease, similar to the observations in the bay mud column, but at a lower rate, suggesting the establishment of the nitrate reducing community in these columns. While the behavior of nitrate in the sandstone columns is similar to that of the bay mud columns, both chlorate and perchlorate treatment columns behave differently than the bay mud columns. For chlorate, its effluent concentration was maintained at ~45 mM throughout the rest of the experiment, which suggest that a sizable DPRM community was likely not established even by the end of the experiment, and the suppressive effects on sulfate reduction is most likely due to its toxicity on SRMs for the entire experiment. As for the perchlorate column, a gradual decrease of the perchlorate concentration was observed following the initial breakthrough. This suggests a slow growth of the DPRMs in this column, but it never reached a significant enough level to completely consume perchlorate by the end of the experiment, contrary to the bay mud column. The transient rebound of sulfide concentration in the perchlorate treated sandstone column is similar to the bay mud column, supporting a possible weaker toxicity effect from perchlorate treatment when compared to chlorate. Note that, the sulfate concentration in the perchlorate treated column never reached the influent level (Fig. 5A), suggesting a sustained level of sulfate reduction. Because sulfide was not detected in the effluent, the produced sulfide was likely re-oxided to elemental sulfur, thus removed from the aqueous phase.

While microbial analysis was not conducted in this study, the difference in the geochemical behavior discussed above can be explained by the differences in the microbial community growth between the bay mud and sandstone columns. Despite the longer experimental duration, the sandstone columns likely experienced much slower rate of establishment for the DPRM community, and the observed geochemical response in the sandstone columns indicates a prolonged period dominated by the direct inhibition effect from chlorate and perchlorate treatments. If the DPRM community was not fully established to completely consume the injected (per)chlorate, its full thermodynamic advantage over SRMs may not be realized even at the end of the experiments. This difference in the rate of DPRM growth and community establishment may be related to the differences in the mineral matrix and the inoculation methods, where the indigenous bay mud incubated under stagnant flow condition may have provided a more suitable environment for microbial growth when compared with the foreign, sterilized sandstone matrix with in-flow inoculation.

5. Conclusion

Biosouring and subsequent desouring experiments were conducted in this study to investigate (1) the effects of nitrate, chlorate and perchlorate treatments on souring control and the underlying mechanisms and (2) the use of galvanic potential measurements for quantitative tracking of sulfide dynamics during the experiments.

Our experiments demonstrated that all three chemicals were effective at suppressing sulfidogenesis. Bio-competitive exclusion seemed to be the main mode which nitrate inhibited sulfate reduction. (Per) chlorate treatments showed multimodal inhibition effects on sulfate reduction. Specifically, our geochemical data suggested that toxicity, direct sulfide oxidation, and bio-competitive exclusion were at work during (per)chlorate treatments. Our results also revealed a possible weaker toxicity/inhibitory effects from perchlorate treatment when compared with chlorate, which warranted further studies. In terms of perchlorate treatment, an integrated approach in which RTM simulation results were coupled to geochemical data to gain additional insights into the interactions between the underlying competing mechanisms of perchlorate was utilized. In all, simulation results point to the toxicity impact of perchlorate as the most important mechanism for this set of perchlorate treatment columns. Galvanic potential monitoring was conducted to evaluate its feasibility for quantitative estimation of sulfide concentrations under different matrix and treatment conditions. The correlations between sulfide concentration and galvanic potential were nearly identical for both sets of columns, indicating insensitivity of this method to matrix and aqueous geochemical conditions. The sulfide-galvanic potential correlation based on our experimental data is close to the theoretical perditions based on the Nernst equation, indicating the feasibility for quantification of sulfide concentrations based on galvanic potential measurements. These results suggest a possible solution for quick, continuous and economical in situ sulfide measurement technology based on, for example, downhole galvanic sensor arrays located at the bottom of boreholes in oil fields. Such an approach would be particularly useful in capturing onset and immediate response to intervention, and to understand the dynamics of sulfur cycling under in-situ thermodynamic conditions. The remnant galvanic response at the end of the experiment suggests the need to design robust electrodes that can function for a long time in the challenging multiphase oil reservoir environments at elevated pressure and temperature conditions.

Acknowledgements

The Energy Biosciences Institute provided funding for this research. We appreciate the bay mud material and the microbial enrichment provided by Anna Engelbrektson and John Coates at UC Berkeley. We thank the editor and the two anonymous reviewers for constructive comments that improved this manuscript. The data presented in this manuscript is available upon request.

References

Baeuerle, M.E., Huttner, W.B., 1986. Chlorate - a potent inhibitor of protein sulfation in intact cells. Biochem. Biophys. Res. Commun. 141, 870–877.

Beauchamp, R.O., Bus, J.S., James, A.P., Boreiko, C.J., Andjelkovich, D.A., 1984. A critical review of the literature on hydrogen sulfide toxicity. Crit. Rev. Toxicol. 13 (1), 25–97.

Brendel, P.J., Luther, G.W., 1995. Development of a gold amalgam voltammetric microelectrode for the determination of dissolved Fe, Mn, O2, and S(-II) in porewaters of marine and freshwater sediments. Environ. Sci. Technol. 29, 751–761.

Callbeck, C.M., Agrawal, A., Voordouw, G., 2013. Acetate production from oil under sulfate-reducing conditions in bioreactors injected with sulfate and nitrate. Appl. Environ. Microbiol. 79, 5059–5068. http://dx.doi.org/10.1128/AEM.01251-13.

Carlson, H., Kuehl, J., Hazra, A., Justice, N., Stoeva, M., Sczesnak, A., Mullan, M., Iavarone, A., Engelbrektson, A., Price, M., Deutschbauer, A., Arkin, A., Coates, J., 2014. Mechanisms of direct inhibition of the respiratory sulfate-reduction pathway by (per)chlorate and nitrate. ISME J. 9 (6), 1295–1305.

Cheng, Y., Hubbard, C.G., Li, L., Bouskill, N.J., Molins, S., Zheng, L., Sonnenthal, E., Conrad, M.E., Engelbrektson, A., Coates, J.D., 2016. A reactive transport model of sulfur cycling as impacted by perchlorate and nitrate treatments. Environ. Sci. Technol. 50 (13), 7010–7018.

Cline, J.D., 1969. Spectrophotometric determination of hydrogen sulfide in natural waters. Limnol. Oceanogr. 14 (3), 454–458.

Coates, J.D., Achenbach, L.A., 2004. Microbial perchlorate reduction: rocket-fueled metabolism. Nat. Rev. Microbiol. 2 (7), 569–580.

Coates, J.D., Michaelidou, U., Bruce, R.A., O'Connor, S.M., Crespi, J.N., Achenbach, L.A., 1999. Ubiquity and diversity of dissimilatory (per)chlorate-reducing bacteria. Appl. Environ. Microbiol. 65 (12), 5234–5241.

Cohen, Y., Metzner, A.B., 1981. Wall effects in laminar flow of fluids through packed beds. AICHE J. 27 (5), 705–715.

Cord-Ruwisch, R., 1985. A quick method for the determination of dissolved and precipitated sulfides incultures of sulfate-reducing bacteria. J. Microbiol. Methods 4, 33–36.

De Gusseme, B., De Schryver, P., De Cooman, M., Verbeken, K., Boeckx, P., Verstraete, W., Boon, N., 2009. Nitrate-reducing, sulfide-oxidizing bacteria as microbial oxidants for

rapid biological sul¢de removal. FEMS Microbiol. Ecol. 67, 151–161.
Druhan, J.L., Steefel, C.I., Molins, S., Williams, K.H., Conrad, M.E., DePaolo, D.J., 2012. Timing the onset of sulfate reduction over multiple subsurface acetate amendments by measurement and modeling of sulfur isotope fractionation. Environ. Sci. Technol. 46 (16), 8895–8902.
Druhan, J.L., Steefel, C.I., Williams, K.H., DePaolo, D.J., 2013. Calcium isotope fractionation in *groundwater*: molecular scale processes influencing field scale behavior. Geochim. Cosmochim. Acta 119, 93–116.
Druhan, J.L., Steefel, C.I., Conrad, M.E., DePaolo, D.J., 2014. A large column analog experiment of stable isotope variations during reactive transport: I. A comprehensive model of sulfur cycling and δ34S fractionation. Geochim. Cosmochim. Acta 124, 366–393.
Engelbrektson, A., et al., 2014. Inhibition of microbial sulfate reduction in a flow-through column system by (per)chlorate treatment. Front. Microbiol. 5, 315.
Fang, Y.L., Yabusaki, S.B., Morrison, S.J., Amonette, J.P., Long, P.E., 2009. Multicomponent reactive transport modeling of uranium bioremediation field experiments. Geochim. Cosmochim. Acta 73, 6029–6051.
Gieg, L.M., Jack, T.R., Foght, J.M., 2011. Biological souring and mitigation in oil reservoirs. Appl. Microbiol. Biotechnol. 92 (2), 263–282.
Gregoire, P., Engelbrektson, A., Hubbard, C.G., Metlagel, Z., Csencsits, R., Auer, M., Conrad, M.E., Thieme, J., Northrup, P., Coates, J.D., 2014. Control of sulfidogenesis through bio-oxidation of H2S coupled to (per)chlorate reduction. Environ. Microbiol. Rep. 6 (6), 558–564.
He, Q., He, Z., Joyner, D.C., Joachimiak, M., Price, M.N., Yang, Z.K., 2010. Impact of elevated nitrate on sulfate-reducing bacteria: a comparative study of *Desulfovibrio vulgaris*. ISME J. 1386–1397.
Hubert, C., 2010. Microbial ecology of oil reservoir souring and its control by nitrate injection. In: Timmis, K. (Ed.), Handbook of Hydrocarbon and Lipid Microbiology. Springer, Berlin, Germany, pp. 2753–2766.
Hubert, C., Voordouw, G., 2007. Oil field souring control by nitrate-reducing Sulfurospirillum spp. that outcompete sulfate-reducing bacteria for organic electron donors. Appl. Environ. Microbiol. 73 (8), 2644–2652.
Jin, Q., Roden, E.E., 2011. Microbial physiology-based model of ethanol metabolism in subsurface sediments. J. Contam. Hydrol. 125, 1–12.
Kapusta, S., Viehbeck, A., Wilhelm, S.M., Hackerman, N., 1983. The anodic oxidation of sulfide on platinum electrodes. J. Electroanal. Chem. 153, 157–174.
Li, L., Steefel, C.I., Williams, K.H., Wilkins, M.J., Hubbard, S.S., 2009. Mineral transformation and biomass accumulation associated with uranium bio-remediation at Rifle, Colorado. Environ. Sci. Technol. 43, 5429–5435.
Li, L., et al., 2017. Expanding the role of reactive transport models in critical zone processes. Earth Sci. Rev. 165, 280–301.
Mehta-Kolte, M.G., Loutey, D., Wang, O., Youngblut, M.D., Hubbard, C.G., Wetmore, K.M., Conrad, M.E., Coates, J.D., 2017. Mechanism of H2S oxidation by the dissimilatory perchlorate-raducing microorganism *Azospira suillum* PS. MBio 8, e02023-16. http://dx.doi.org/10.1128/mBio.02023-16.
Pallud, C., Van Cappellen, P., 2006. Kinetics of microbial sulfate reduction in estuarine sediments. Geochim. Cosmochim. Acta 70, 1148–1162.
Personna, Y.R., Ntarlagiannis, D., Slater, L., Yee, N., O'Brien, M., Hubbard, S., 2008. Spectral induced polarization and electrodic potential monitoring of microbially mediated iron sulfide transformations. J. Geophys. Res. 113, G02020. http://dx.doi.org/10.1029/2007JG000614.
Porter, D., Roychoudhury, A.N., Cowan, D., 2007. Dissimilatory sulfate reduction in hypersaline coastal pans: activity across a salinity gradient. Geochim. Cosmochim. Acta 71, 5102–5116.
Postgate, J.R., 1952. Competitive and non-competitive inhibitors of bacterial sulphate reduction. J. Gen. Microbiol. 6, 128–142.
Reiffenstein, R.J., Hulbert, W.C., Roth, S.H., 1992. Toxicology of hydrogen sulfide. Annu. Rev. Pharmacol. Toxicol. 32, 109–134.
Rittman, B.E., MaCarty, P.L., 2001. Environmental Biotechnology: Principles and Applications. 2001 McGraw-Hill, New York.
Steefel, C.I., Maher, K., 2009. Fluid-rock interaction: a reactive transport approach. Rev. Mineral. Geochem. 70 (1), 485–532.
Steefel, C.I., Druhan, J.L., Maher, K., 2014. Modeling coupled chemical and isotopic equilibration rates. Procedia Earth Planet. Sci. 10, 208–217.
Stock, J., Orna, M.V., 1989. Electrochemistry, Past and Present. American Chemical Society, Columbus, Ohio.
Sunde, E., Torsvik, T., 2005. Microbial control of hydrogen sulfide production in oil reservoirs. In: Ollivier, B., Magot, M. (Eds.), Petroleum Microbiology. ASM Press, Washington DC, pp. 201–213.
Voordouw, G., Grigoryan, A.A., Lambo, A., Lin, S., Park, H.S., Jack, T.R., 2009. Sulfide remediation by pulsed injection of nitrate into a low temperature Canadian heavy oil reservoir. Environ. Sci. Technol. 43, 9512–9518.
Williams, K.H., Hubbard, S.S., Banfield, J.F., 2007. Galvanic interpretation of self-potential signals associated with microbial sulfate-reduction. J. Geophys. Res. 112, G03019. http://dx.doi.org/10.1029/2007JG000440. (002007).
Williams, K.H., N'Guessan, A.L., Druhan, J., Long, P.E., Hubbard, S.S., Lovely, D.R., Banfield, J.F., 2010. Electrodic voltages accompanying stimulated bioremediation of a uranium - contaminated aquifer. J. Geophys. Res. 115, G00G05. http://dx.doi.org/10.1029/2009JG001142. (002010).
Yabusaki, S.B., Fang, Y., Williams, K.H., Murray, C.J., Ward, A.L., Dayvault, R.D., et al., 2011. Variably saturated flow and multicomponent biogeochemical reactive transport modeling of a uranium bioremediation field experiment. J. Contam. Hydrol. 126, 271–290.
Zhang, C., Ntarlagiannis, D., Slater, L., Doherty, R., 2010. Monitoring microbial sulfate reduction in porous media using multipurpose electrodes. J. Geophys. Res. 115, G00G09. http://dx.doi.org/10.1029/2009JG001157.